COMPRESSIVE PUSHBROOM AND WHISKBROOM SENSING FOR HYPERSPECTRAL REMOTE-SENSING IMAGING

James E. Fowler

Department of Electrical and Computer Engineering, Geosystems Research Institute,
Mississippi State University, USA

ABSTRACT

Most existing architectures for the compressive acquisition of hyperspectral imagery—which perform dimensionality reduction simultaneously with image acquisition—have focused on framing designs which require the entire spatial extent of the image be available at once to the sensor. On the other hand, hyperspectral imagery in remote-sensing applications is frequently acquired with a pushbroom or whiskbroom sensing paradigm which—incorporating line-based or pixel-based scanning, respectively—exploits the motion inherent in an airborne or satellite-borne sensing platform to acquire the image. Such pushbroom and whiskbroom sensing architectures are proposed for the compressive acquisition of hyperspectral imagery. Additionally, the necessity of employing multiple sensor arrays in order to sense a broad spectrum, including the infrared regime, is considered.

Index Terms— compressed sensing, hyperspectral imagery, remote sensing

1. INTRODUCTION

The recent advent of compressed sensing (CS) has served as the impetus for a number of CS-based image-sensor designs which effectively apply linear projections in the optical domain such that dimensionality reduction occurs simultaneously with image sensing and acquisition. While initial designs focused on the compressive acquisition of single-band, or grayscale, imagery (e.g., [1–4]), subsequent work (e.g., [5–10]) has considered the compressive acquisition across a multitude of spectral bands, particularly for the case of hyperspectral imagery—see [11] for an overview. In brief, a hyperspectral image is a volumetric (or 3D) imagery dataset consisting of a spatial array of vector-valued pixels. Each hyperspectral pixel vector typically consists of several hundred optical-spectrum samples from contiguous wavelength channels (bands), typically ranging from the near-ultraviolet to the short- or long-wave infrared.

While hyperspectral imagery has been employed in a wide range of application settings, there is great interest in hyperspectral remote sensing of the Earth's surface due to the fact that the large spectral resolution of the resulting imagery permits detecting, distinguishing, and identifying materials remotely over long distances [12]. Typically, hyperspectral remote-sensing sensors are mounted on some type of airborne or satellite-borne platform. While some such platforms are static—such as an aerostat or geosynchronous satellite—and, consequently, permit imaging only a fixed spatial region on the Earth, more commonly hyperspectral remote-sensing sensors reside on moving airplanes or satellites and image vast spatial areas of the Earth along the platform flight line. As a consequence, hyperspectral sensors for remote sensing are often of a scanning design that acquires individual pixels—or entire lines of pixels—sequentially, exploiting the motion of the sensor platform to provide the requisite down-track scanning [12]. Such scanning designs are typically categorized as "whiskbroom" or "pushbroom" according to whether they employ pixel-based or line-based scanning, respectively [12].

Most existing designs for compressive hyperspectral sensors (i.e., [5–10]), however, have focused on "framing" acquisition. In a framing sensor, the entire 2D spatial extent of the scene is imaged at once. In remote sensing, such framing sensors best suit aerostat or geosynchronous platforms. Consequently, there is need for compressive sensor designs that are based on pushbroom and whiskbroom scanning in order to permit compressive hyperspectral image acquisition from moving airplane and satellite platforms.

In this paper, we propose two conceptual designs for compressive hyperspectral remote-sensing sensors, one for each of the pushbroom and whiskbroom scanning paradigms. We first overview existing compressive hyperspectral sensing architectures next, subsequently presenting our proposed pushbroom and whiskbroom designs in Secs. 3 and 4, respectively. We then consider the issue of imaging across a broad spectral range using multiple sensor materials in Sec. 5 before making concluding remarks in Sec. 6.

2. BACKGROUND

Perhaps the most widely invoked architecture for compressive imaging is the well-known "single-pixel camera" (SPC) [1–4] depicted in Fig. 1 and used for the acquisition of a 2D grayscale (i.e, single-band or panchromatic) image. In essence, the SPC uses a digital micromirror device (DMD) to optically perform an inner product between the measurement pattern on the DMD and the image being acquired, the photosensor outputting the corresponding measurement value as an analog voltage. The measurement pattern on the DMD is changed and the process repeated until the desired number of measurements is obtained, implying that the imaged scene remains static during the time it takes to acquire the consecutive measurements.

A number of compressive hyperspectral sensors have been based on the SPC framework; notably, [5] simply replaces the single photosensor in Fig. 1 with a spectrometer, which produces a separate measurement value for each spectral band. The spectrometer is implemented as a spectral dispersion followed by a linear array of photosensors. Effectively, this architecture applies the same compressive measurement process simultaneously and in parallel to multiple spectral bands; consequently, the acquisition is compressive in the spatial direction only.

An alternative approach—that of applying compressive acquisition exclusively in the spectral direction—was adopted in the coded-aperture snapshot spectral imager (CASSI) [6, 7] which uses spectral shearing of a hyperspectral image cube along with a coded aperture to effectuate a compressive projection of each spectral pixel in the

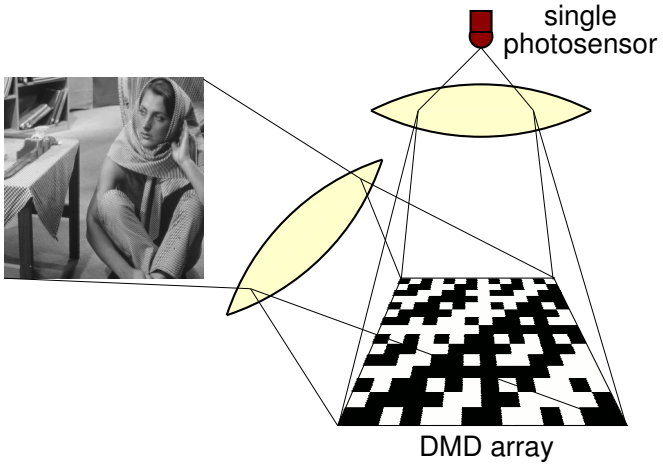

Fig. 1. The SPC [1–4] for the compressive acquisition of single-band image (figure adapted from [21]).

image; multiple snapshots with distinct aperture codes [8] yield multiple measurements for each pixel vector. It should be noted that the CASSI architecture requires an array of photosensors of the same size as the spatial dimensions of the image acquired, in contrast to the simpler linear array employed in [5]. Several variants of the CASSI architecture have been proposed, including a single-disperser design [9] as well as a DMD-based implementation [8].

Finally, [10] proposes hyperspectral image acquisition that is compressive in both the spatial as well as spectral directions. In short, the compressive hyperspectral imaging by separable spectral and spatial operators (CHISSS) system replaces the single photosensor in the traditional SPC architecture with a separate spectral-encoding subsystem; this spectral encoding will be described in depth in Sec. 4 later.

One characteristic common to all of the aforementioned systems is their reliance on framing acquisition; i.e., they image the entire 2D spatial extent of the acquired scene at once. However, many remote-sensing applications require the use of sensors which acquire imagery using a spatial-scanning process due to their placement on moving airborne or satellite-borne platforms. Consequently, we propose architectures for compressive pushbroom and whiskbroom sensing in the sequel. Like [6], the proposed designs are compressive in the spectral direction only; however, the pushbroom or whiskbroom scanning eliminates the need to access the entire spatial extent of the image as the framing design of [6] does. We note also that spectrally compressive acquisition permits certain operations (e.g., anomaly detection [13, 14], classification [15–18], and target detection [14, 15, 19, 20]) to be conducted without requiring dataset reconstruction.

3. PUSHBROOM SENSING

The pushbroom paradigm is a popular scanning strategy among traditional hyperspectral sensors for remote sensing, being used by the HYDICE, CASI, and Hyperion systems, among others [12, 22]. The hallmark of pushbroom sensing is that an entire line, or row, of the hyperspectral imagery is acquired at once, with the motion of the airborne or satellite-borne platform providing the down-track scanning [12].

A pushbroom architecture for the compressive acquisition of hyperspectral imagery is depicted conceptually in Fig. 2. This sensor is centered around a DMD, while a spectral-splitting device (e.g., a prism) spreads a single line from a slit aperture across the DMD, the reflections of which are focused onto a line of photosensors through a cylindrical lens.

Mathematically, let the current line from the hyperspectral image contain M pixels, $\mathbf{x}_m$, $1 \leq m \leq M$, with each pixel consisting of N spectral bands; i.e., $\mathbf{x}_m \in \Re^N$. The compressive acquisition of pixel $\mathbf{x}_m$ produces measurement vector $\mathbf{y}_m = \mathbf{P}_m^T \mathbf{x}_m$, where compressive measurement matrix $\mathbf{P}_m$ is of size $N \times K$, $K \ll N$, and $\mathbf{y}_m \in \Re^K$. Here, we assume each hyperspectral pixel vector $\mathbf{x}_m$ possesses its own measurement matrix $\mathbf{P}_m$, although the same matrix could be used for all pixels[1].

In the pushbroom sensor of Fig. 2, each column of the DMD performs the inner product of the corresponding hyperspectral pixel vector $\mathbf{x}_m$ against a particular column of $\mathbf{P}_m$. Specifically, at time k, column k of $\mathbf{P}_m$ is placed on column m of the DMD so that the corresponding photosensor records vector component k of $\mathbf{y}_m$; this process is repeated in quick succession for $1 \leq k \leq K$, thusly assembling the K-dimensional projected vector $\mathbf{y}_m$ from successive reads of photosensor m in the linear array. This process is conducted simultaneously on all M columns of the DMD, using for each DMD column its corresponding $\mathbf{P}_m$ matrix, such that $\mathbf{y}_m$ is acquired for all pixels of a single image row simultaneously; afterwards, the sensor advances to the next line, and the process is repeated. We note that the DMD has size $N \times M$, while the linear array of photosensors is $1 \times M$.

The primary disadvantage of the proposed pushbroom architecture is the need for conducting the K measurements successively. Although modern DMDs are capable of fast operation (DMDs on the order of 0.1–1 MHz are commercially available), the successive measurement process effectively cuts the dwell time[2] of the sensor by a factor of K as compared to a traditional, non-compressive pushbroom sensor. However, the proposed architecture comes with the advantage that only a single, 1D linear array of K photosensors is required, whereas traditional pushbroom sensors require a 2D array of photosensors of size $M \times N$. Depending on the cost per photosensor, the compressive pushbroom architecture of Fig. 2 may offer the possibility of dramatically reduced sensor cost, particularly for imaging outside of the visible range—see Sec. 5 below for more discussion on this issue.

Finally, we note that [26] suggests pushbroom acquisition be effectuated by preceding the SPC of Fig. 1 with a diffractive element. This would result in measurements that are compressive across a 2D spatial-spectral slice of a hyperspectral volume; however, the dwell time is reduced by a factor of MK as compared to a non-compressive pushbroom sensor for K spectral bands and M pixels in the pushbroom line.

4. WHISKBROOM SENSING

In addition to pushbroom, the other scanning paradigm in popular use in hyperspectral remote sensing is the whiskbroom scan, which is built on the imaging of a single pixel, or spatial location, at a time. A rotating mirror is employed to sweep out a scan line perpendicular to the motion of the sensor platform [12, 22]. As with the pushbroom

[1] Certain algorithms (e.g., [23, 24]) for the reconstruction of $\mathbf{x}_m$ from $\mathbf{y}_m$ require the use of a different measurement matrix per vector.

[2] The dwell time is the amount of time a sensor element remains over a particular spatial location that it is imaging. A longer dwell time results in increased collection of photons and a correspondingly larger signal-to-noise ratio [12, 25].

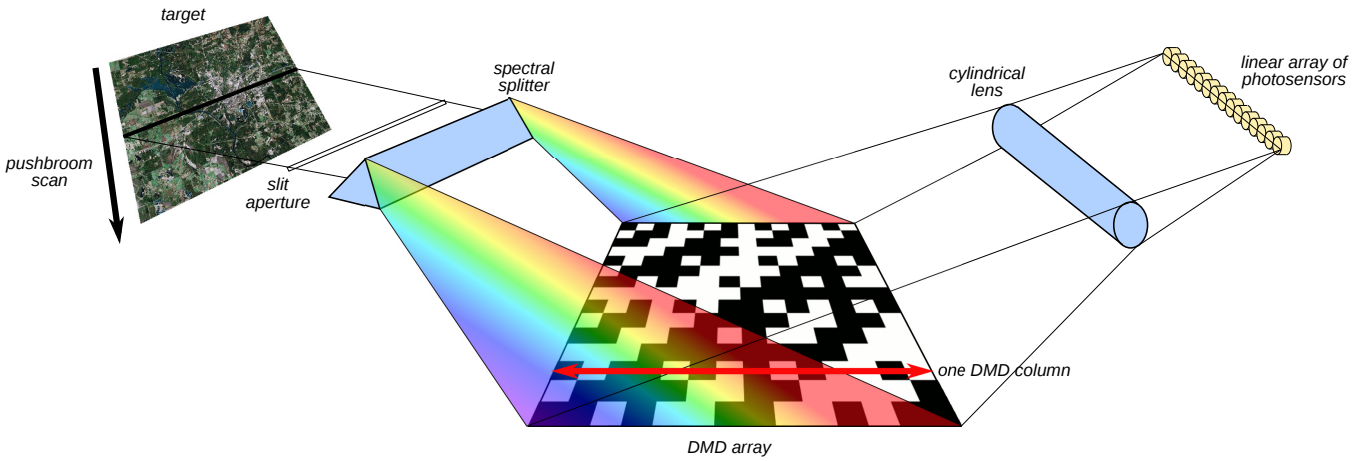

Fig. 2. A compressive pushbroom hyperspectral sensor.

scan, the whiskbroom scan relies on the motion of the airborne or satellite-borne sensor platform to yield down-track scanning. Traditional hyperspectral sensors that use whiskbroom scanning include AVIRIS and HyMap [12, 22].

A whiskbroom architecture for the compressive acquisition of hyperspectral imagery is depicted conceptually in Fig. 3. As with the pushbroom architecture of Fig. 2, this whiskbroom sensor is based on a DMD used in conjunction with a spectral splitter. Effectively, the architecture shown in Fig. 3 is the spectral encoder proposed for the separable spatial-spectral compressive imager in [10]; specifically, the SPC used in [10] for spatial encoding has been replaced with a pinhole aperture and a rotating scan mirror to effectuate whiskbroom scanning.

In Fig. 3, for a given spatial location, the light emitting from the pinhole aperture is dispersed by the spectral splitter into a spectral line which is spread across the DMD as parallel rays by a cylindrical lens. Consequently, each DMD row corresponds to a different spectral band; meanwhile, a different measurement pattern is placed on each DMD column. The second cylindrical lens sums across each DMD column, providing a separate measurement value to each photosensor in the linear array. The rotating scan mirror then advances to the next pixel in the line, while the platform motion advances the scan to the next line.

Mathematically, let the current N-band hyperspectral pixel vector being imaged be $\mathbf{x} \in \Re^N$; the measurement process is again $\mathbf{y} = \mathbf{P}^T\mathbf{x}$, where $\mathbf{y} \in \Re^K$, and $\mathbf{P}$ is of size $N \times K$. Column k of the DMD performs the inner product of $\mathbf{x}$ with column k of $\mathbf{P}$, yielding vector component k of $\mathbf{y}$ on photosensor k. Consequently, the DMD has N rows and K columns; vector $\mathbf{y}$ is read from the k photosensors of the $1 \times K$ linear array at once. We note that, if the same matrix $\mathbf{P}$ were applied to acquire each pixel vector, the measurement pattern on the DMD would remain static; in this case, a fixed coded aperture could be used instead of the DMD. However, use of a DMD permits a different measurement matrix for each vector[3].

The proposed compressive whiskbroom architecture of Fig. 3 offers the advantage over the compressive pushbroom architecture of Fig. 2 in that all K measurements for a pixel are acquired simultaneously, obviating the need for the successive acquisition used in the pushbroom system. Consequently, the compressive whiskbroom sensor of Fig. 3 has the same dwell time as a comparable traditional whiskbroom sensor (which is, however, typically much less than that of an equivalent non-compressive pushbroom architecture). The disadvantages of the compressive whiskbroom architecture are those inherited from the traditional whiskbroom paradigm, including geometrical issues stemming from platform stability and mechanical scanning [12].

[3]Again, as may be required by certain reconstruction algorithms such as [23, 24].

5. SENSING OF LONGER WAVELENGTHS

Existing implementations and conceptual designs for compressive hyperspectral sensors (e.g., [5, 6, 8–10]) assume that a single linear or 2D photosensor array is used. This consequently implies that a single detector material—typically, silicon—is employed, thereby limiting the spectral range of acquisition. While the spectral range of silicon—0.3 μm to 1.0 μm—encompasses the entire visible range as well as some of the ultraviolet and near-infrared spectra [12], many applications in remote sensing make use of the spectrum at longer wavelengths.

Typically, traditional hyperspectral sensors achieve operation over a broad spectral range by imaging onto separate sensor arrays, each constructed from a different material. For example, the AVIRIS platform employs four distinct sensor arrays, one made from silicon (Si) detectors, and the other three from indium antimonide (InSb) detectors [27]. A similar strategy can be adopted for the pushbroom and whiskbroom architectures proposed here.

Specifically, Fig. 4 illustrates how the linear photosensor array used in the whiskbroom sensor of Fig. 3 can be replaced by a beam splitter followed by separate photosensor arrays tailored for acquiring different spectral ranges. Fig. 4 shows specifically acquisition in the visible as well as near-infrared (NIR) regimes accomplished with silicon-based photosensors, while acquisition in the short-wave infrared (SWIR) uses indium gallium arsenide (InGaAs) detectors. Mathematically, this multiband-acquisition process functions as follows. Consider the sensing of measurement y_k, the k^{th} component of measurement vector $\mathbf{y}$. Column k of the DMD in Fig. 3 performs the inner product of hyperspectral pixel vector $\mathbf{x}$ with $\mathbf{p}_k$, column k of measurement matrix $\mathbf{P}$. However, the Si and InGaAs detectors measure only $y'_k = \mathbf{p}_k^T \begin{bmatrix} \mathbf{x}' \\ \mathbf{0} \end{bmatrix}$ and $y''_k = \mathbf{p}_k^T \begin{bmatrix} \mathbf{0} \\ \mathbf{x}'' \end{bmatrix}$, respectively, where the limited spectral ranges of the photosensors effectively split $\mathbf{x}$ as

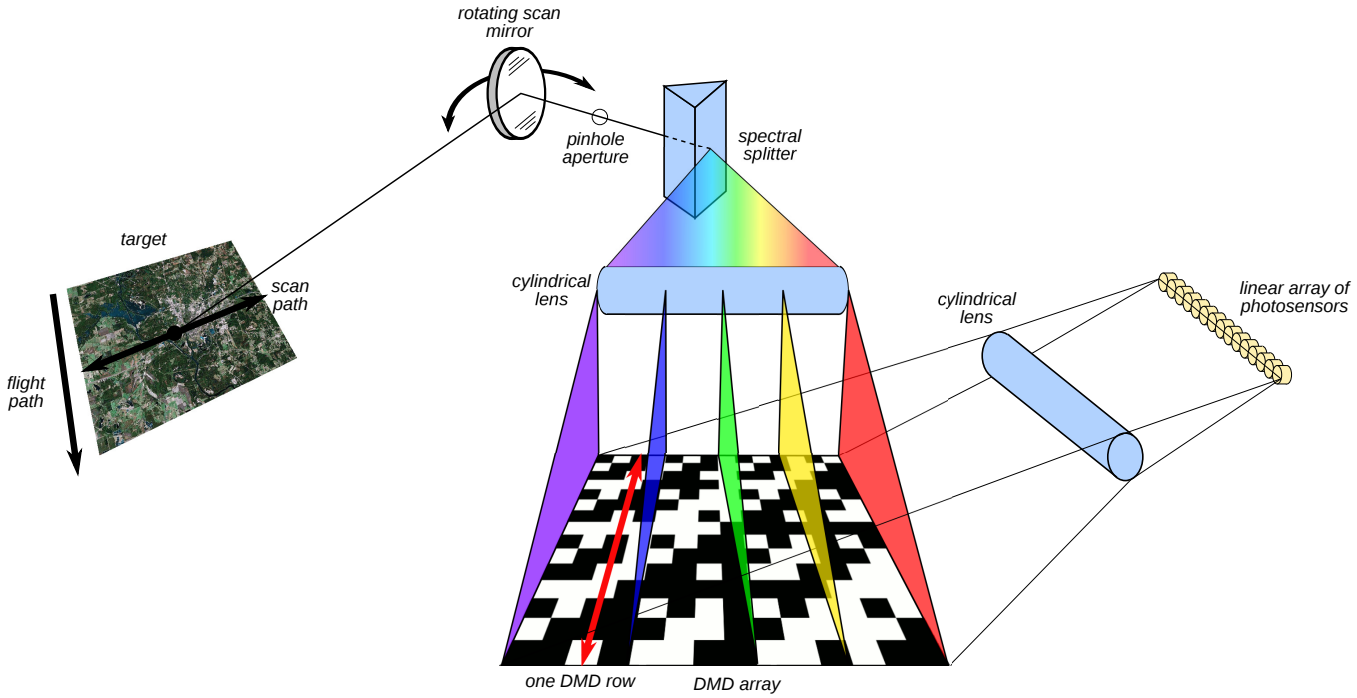

Fig. 3. A compressive whiskbroom hyperspectral sensor.

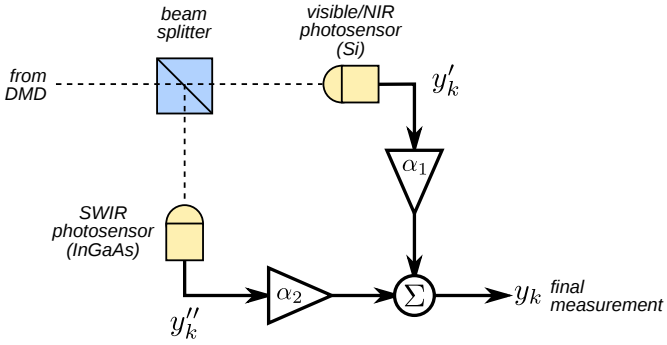

Fig. 4. Increasing the spectral range of the whiskbroom sensor by splitting the DMD output to sensors constructed from different materials (illustrated for sensor k of a $1 \times K$ linear photosensor array for each material).

$\mathbf{x} = \begin{bmatrix} \mathbf{x}' \\ \mathbf{x}'' \end{bmatrix}$. Consequently, to form the final measurement y_k, an analog summer adds y'_k and y''_k electrically, $y_k = \alpha_1 y'_k + \alpha_2 y''_k$, where gain parameters α_1 and α_2 compensate for possible variances in relative photoelectric sensitivities between the two sensor materials. Additional beam splitters and sensor arrays could be added to Fig. 4 in order to employ more than two sensor materials, thereby extending the sensor range into even longer wavelengths. Additionally, Fig. 4 could be used, as is, with the pushbroom architecture of Fig. 2 to extend its spectral range as well.

We note that, although existing designs for compressive hyperspectral sensors (e.g., [5–10]) focus on just a single photosensor array, the basic strategy of Fig. 4 could be applied to these existing designs as well. However, imaging beyond the near-infrared unfortunately requires materials that are comparatively exotic and, consequently, costly, as such sensors lack the large commercial market with which silicon is blessed. Additionally, sensors for longer wavelengths typically operate at extremely low temperatures, requiring a significant cost to achieve the required cooling. Consequently, compressive hyperspectral sensor designs that require 2D sensor arrays that are the same size as the spatial dimensions of the image would be significantly more costly than the simple 1D linear arrays used in the pushbroom and whiskbroom design proposed here. Such is the case of the well-known CASSI [6, 7] architecture and its variants [8, 9].

6. CONCLUSION

In this paper, we proposed designs for compressive hyperspectral sensors specifically intended for the pushbroom and whiskbroom scanning that are commonly used for airborne and satellite-borne remote sensing. These designs stand in contrast to previous architectures which instead employ a framing acquisition and are thus limited to static (aerostat or geosynchronous) imaging. We also considered the necessity of employing multiple sensor arrays constructed from different materials in order to cover a broad spectrum ranging well into the infrared regime. Given that such infrared sensors require substantial cost due to comparatively exotic sensor material as well as significant cooling burden, the proposed designs have the advantage that only a 1D linear array of photosensors need be implemented, while competing designs—namely CASSI [6, 7] and its variants [8, 9]—require a 2D array of sensors matching the spatial resolution, thereby entailing potentially prohibitive cost.

7. REFERENCES

[1] D. Takhar, J. N. Laska, M. B. Wakin, M. F. Duarte, D. Baron, S. Sarvotham, K. F. Kelly, and R. G. Baraniuk, "A new compressive imaging camera architecture using optical-domain compression," in *Computational Imaging IV*, C. A. Bouman, E. L. Miller, and I. Pollak, Eds. San Jose, CA: Proc. SPIE 6065, January 2006, p. 606509.

[2] M. B. Wakin, J. N. Laska, M. F. Duarte, D. Baron, S. Sarvotham, D. Takhar, K. F. Kelly, and R. G. Baraniuk, "An architecture for compressive imaging," in *Proceedings of the International Conference on Image Processing*, Atlanta, GA, October 2006, pp. 1273–1276.

[3] ——, "Compressive imaging for video representation and coding," in *Proceedings of the Picture Coding Symposium*, Beijing, China, April 2006.

[4] M. F. Duarte, M. A. Davenport, D. Takhar, J. N. Laska, T. Sun, K. F. Kelly, and R. G. Baraniuk, "Single-pixel imaging via compressive sampling," *IEEE Signal Processing Magazine*, vol. 25, no. 2, pp. 83–91, March 2008.

[5] T. Sun and K. Kelly, "Compressive sensing hyperspectral imager," in *Computational Optical Sensing and Imaging*, San Jose, CA, October 2009, p. CTuA5.

[6] M. E. Gehm, R. John, D. J. Brady, R. M. Willett, and T. J. Schulz, "Single-shot compressive spectral imaging with a dual-disperser architecture," *Optics Express*, vol. 15, no. 21, pp. 14 013–14 027, October 2007.

[7] G. R. Arce, D. J. Brady, L. Carin, H. Arguello, and D. S. Kittle, "Compressive coded aperture spectral imaging," *IEEE Signal Processing Magazine*, vol. 31, no. 1, pp. 105–115, January 2014.

[8] Y. Wu, I. O. Mirza, G. R. Arce, and D. W. Prather, "Development of a digital-micromirror-device-based multishot snapshot spectral imaging system," *Optics Letters*, vol. 36, no. 14, pp. 2692–2694, July 2011.

[9] A. Wagadarikar, R. John, R. Willett, and D. Brady, "Single disperser design for coded aperture snapshot spectral imaging," *Applied Optics*, vol. 47, no. 10, pp. B44–B51, April 2008.

[10] Y. August, C. Vachman, Y. Rivenson, and A. Stern, "Compressive hyperspectral imaging by random separable projections in both the spatial and the spectral domains," *Applied Optics*, vol. 52, no. 10, pp. D46–D54, April 2013.

[11] R. M. Willett, M. F. Duarte, M. A. Davenport, and R. G. Baraniuk, "Sparsity and structure in hyperspectral imaging," *IEEE Signal Processing Magazine*, vol. 31, no. 1, pp. 116–126, January 2014.

[12] J. P. Kerekes and J. R. Schott, "Hyperspectral imaging systems," in *Hyperspectral Data Exploitation: Theory and Applications*, C.-I. Chang, Ed. Hoboken, NJ: John Wiley & Sons, Inc., 2007, ch. 12, pp. 19–45.

[13] J. E. Fowler and Q. Du, "Anomaly detection and reconstruction from random projections," *IEEE Transactions on Image Processing*, vol. 21, no. 1, pp. 184–195, January 2012.

[14] K. Krishnamurthy, R. Willett, and M. Raginsky, "Target detection performance bounds in compressive imaging," *EURASIP Journal on Advances in Signal Processing*, vol. 2012, no. 1, September 2012.

[15] M. A. Davenport, P. T. Boufounos, M. B. Wakin, and R. G. Baraniuk, "Signal processing with compressive measurements," *IEEE Journal of Selected Topics in Signal Processing*, vol. 4, no. 2, pp. 445–460, April 2010.

[16] W. Li, S. Prasad, and J. E. Fowler, "Classification and reconstruction from random projections for hyperspectral imagery," *IEEE Transactions on Geoscience and Remote Sensing*, vol. 51, no. 2, pp. 833–843, February 2013.

[17] M. A. Davenport, M. F. Duarte, M. B. Wakin, J. N. Laska, D. Takhar, K. F. Kelly, and R. G. Baraniuk, "The smashed filter for compressive classification and target recognition," in *Computational Imaging V*. San Jose, CA: Proc. SPIE 6498, January 2007, p. 64980H.

[18] J. Haupt, R. Castro, R. Nowak, G. Fudge, and A. Yeh, "Compressive sampling for signal classification," in *Proceedings of the 40th Asilomar Conference on Signals, Systems, and Computers*, Pacific Grove, CA, October 2006, pp. 1430–1434.

[19] K. Krishnamurthy, M. Raginsky, and R. Willett, "Hyperspectral target detection from incoherent projections: Nonequiprobable targets and inhomogeneous SNR," in *Proceedings of the International Conference on Image Processing*, Hong Kong, September 2010, pp. 1357–1360.

[20] Q. Du, J. E. Fowler, and B. Ma, "Random-projection-based dimensionality reduction and decision fusion for hyperspectral target detection," in *Proceedings of the International Geoscience and Remote Sensing Symposium*, Vancouver, Canada, July 2011, pp. 1790–1793.

[21] J. E. Fowler, S. Mun, and E. W. Tramel, "Block-based compressed sensing of images and video," *Foundations and Trends in Signal Processing*, vol. 4, no. 4, pp. 297–416, March 2012.

[22] T. M. Lillesand, R. W. Kiefer, and J. W. Chipman, *Remote Sensing and Image Interpretation*, 6th ed. Hoboken, NJ: John Wiley & Sons, Inc., 2008.

[23] J. E. Fowler, "Compressive-projection principal component analysis," *IEEE Transactions on Image Processing*, vol. 18, no. 10, pp. 2230–2242, October 2009.

[24] H. Qi and S. M. Hughes, "Invariance of principal components under low-dimensional random projection of the data," in *Proceedings of the International Conference on Image Processing*, Orlando, FL, October 2012, pp. 937–940.

[25] J. B. Campbell and R. H. Wynne, *Introduction to Remote Sensing*, 5th ed. New York: The Guilford Press, 2011.

[26] G. Coluccia, S. K. Kuiteing, A. Abrardo, M. Barni, and E. Magli, "Progressive compressed sensing and reconstruction of multidimensional signals using hybrid transform/prediction sparsity model," *IEEE Journal on Emerging and Selected Topics in Circuits and Systems*, vol. 2, no. 3, pp. 340–352, September 2012.

[27] R. O. Green, M. L. Eastwood, T. G. C. Charles M. Sarture, M. Aronsson, B. J. Chippendale, J. A. Faust, B. E. Pavri, C. J. Chovit, M. Solis, M. R. Olah, and O. Williams, "Imaging spectroscopy and the airborne visible/infrared imaging spectrometer (AVIRIS)," *Remote Sensing of Environment*, vol. 65, no. 3, pp. 227–248, September 1998.